Materials Science and Engineering C 33 (2013) 4384–4391

Contents lists available at ScienceDirect

Materials Science and Engineering C

journal homepage: www.elsevier.com/locate/msec

Creating "hotels" for cells by electrospinning honeycomb-like polymeric structures

T. Liang, S. Mahalingam, M. Edirisinghe *

Department of Mechanical Engineering, University College London, Torrington Place, London WC1E 7JE, UK

ARTICLE INFO

Article history:
Received 18 April 2013
Received in revised form 28 May 2013
Accepted 22 June 2013
Available online 1 July 2013

Keywords:
Nanofibres
Honeycomb
Self-assembly
Electrospinning
Polymer

ABSTRACT

It is well established that three-dimensional honeycomb-like nanofibrous structures enhance cell activity. In this work, we report that electrospun polymer nanofibres self-assemble into three-dimensional honeycomb-like structures. The underlying mechanism is studied by varying the polymer solution concentration, collecting substrates and working distance. The polymer solution concentration has a significant effect on the size of the electrospun nanofibres. The collection substrate and working distance affect the electric field strength, the evaporation of solvent and the discharging of nanofibres and consequently these two had a significant influence on the self-assembly of nanofibres.

1. Introduction

Nanofibres and nanofibrous structures have received much attention recently for their potential applications in many areas [1]. The high surface area to volume ratio of the materials renders applications in electronics, optical devices, batteries and filtration [2–10]. Moreover, they are promising candidates for the bioengineering community for the construction of scaffolds for tissue engineering to mimic the structural and functional profile of the materials found in extracellular matrices [11,12]. In fact, biomedical application of nanofibres and nanofibrous structures is expanding even to drug release, artificial organs, wound healing and vascular grafts [13,14]. Scaffolds which have a honeycomb-like structure have shown to be excellent for differentiation and proliferation of osteoblast cells. The interconnectivity of voids available in these structures is ideal for tissue ingrowth [15] and along with the very high surface area to volume ratio of the nanofibres enhances cell adhesion [12]. In addition, honeycomb-like structures promote uniform cell distribution and provide a stimulating environment for the successful regeneration of tissues [15].

The microstructures of tissue engineering scaffolds play important roles in controlling cellular behaviour [16]. Honeycomb structures have well defined unidirectional channels with various geometrical (triangular, circular, square, polygonal) cross-sections. These structures yield a high permeability throughout the longitudinal direction of the component [17]. It has been reported that honeycomb scaffolds are a suitable carrier for various 3-D cell cultures [18]. Further, it has been demonstrated that the geometry of the scaffold is crucial for vasculature induction and bone formation. It was also reported that honeycomb shaped hydroxyapatite tunnels, with a pore size of 300–400 μm, directly induced bone formation [19], and in the present work we aim to mimic the creation of such structures. In addition, the wall of honeycomb scaffolds may promote the adherence and deposition of cells and create a different environment from those in two-dimensional plastic dishes or hydrogels [20]. Recently, it has been reported that creating gradients in a porous scaffold may induce faster angiogenesis than that in hydrogels, as cells migrate more readily into the porous structure [21]. Gradients along the pitch and web thickness in the radial or axial directions can be made in honeycomb structures for cell attachment [17]. Moreover, these structures have mechanical stability under various physical and chemical conditions. This will help in the exchange of nutrients and waste products between the honeycomb membranes without deformation or collapse. Overall 3-D honeycomb structures can provide the natural extracellular matrix environment with complex mechanical and biochemical interplay as within living systems [15]. This is the rationale behind naming these structures as "hotels" for cells.

Electrospinning is a well-established technique for forming continuous fibres in the nano- to micro-scale range. Although it is more than several decades since its discovery, it has attracted the attention of many researchers in the last two decades due to its easy utilisation for the fabrication of polymeric fibres from natural or synthetic materials [1,14]. In the electrospinning process, a polymer solution held by its surface tension at the end of the nozzle is subjected to an electric field and an electric charge is induced on the liquid surface due to this. When the electric field reaches a critical value, the electric forces overcome the surface tension forces. Eventually, a fine jet is emitted from the apex of the liquid cone and the jet undergoes whipping or

* Corresponding author. Tel.: +44 20 76793920.
E-mail address: m.edirisinghe@ucl.ac.uk (M. Edirisinghe).

0928-4931/$ – see front matter © 2013 Elsevier B.V. All rights reserved.
http://dx.doi.org/10.1016/j.msec.2013.06.036

Table 1
Physical properties of PEO solutions and distilled water used in the experiments.

Solution	Surface tension (mN/m)	Density (kg/m^3)	Viscosity (mPa s)	Electrical conductivity (mS/m)	Forming time (s)
Distilled water	72 ± 1.1	1026 ± 0.8	1.3 ± 0.1	1.2 ± 0.1	–
12 wt.%	68 ± 1.3	1045 ± 1.1	1128 ± 23	21.0 ± 1	1440
13 wt.%	68 ± 1.0	1049 ± 0.9	1631 ± 22	21.8 ± 1	1200
14 wt.%	69 ± 1.6	1050 ± 1.4	1650 ± 33	22.0 ± 1	1020
15 wt.%	71 ± 3.7	1053 ± 1.0	2666 ± 53	25.0 ± 2	720

bending instabilities followed by evaporation of solvent producing electrospun fibres on a substrate [22,23]. This is different to the electrospraying process where the instability of the jet breaks up into fine monodispersed droplets [24]. The outcome of a polymer electrospinning process is influenced by many interrelated variables, including operating parameters, such as applied voltage, flow rate, collection distance (distance between nozzle end and collection point), nozzle design, physical nature and geometry of the collecting substrate as well as material parameters including solution concentration, molecular chain length, viscosity, surface tension and electrical conductivity [25–30].

Electrospinning is not well known to form 3-D nanofibrous structures. However, a few researchers have reported that 3-D structures can be formed on conventional flat substrates. Deitzel et al. [31] showed that the 3-D fibrous structures are formed by lowering the polymer solution viscosity and increasing the spinning voltage. The formation of this unusual structure arises due to electrostatic charge build up in the fibre beads and the fibres that prevent the newly electrospun fibres from lying directly on the mats. A similar observation was found by Thandavamoorthy et al. [32] who attributed the formation of 3-D honeycomb-like nanofibrous structures to the characteristics of the collector. Despite these reports there is not much research on what conditions are required to form such three-dimensional nanofibrous structures on conventional flat substrates and how these are formed still remains rather unclear. The present work elucidates the formation of 3-D honeycomb-like nanofibrous structures on conventional flat substrates by electrospinning. The relationship between the concentration of the polymer solution and the self-assembly of the nanofibres to form such structures is explained. Further, the working distance and the effect of the substrate are investigated to uncover further information on the formation of these structures.

2. Experimental details

2.1. Materials and solutions

The polymer solutions used in electrospinning experiments were prepared using polyethylene oxide (PEO, molecular weight 200,000 g/mol) supplied from Sigma-Aldrich (UK). This material was dissolved in distilled water to make concentrations of 12 wt.%, 13 wt.%, 14 wt.% and 15 wt.%. The polymer solutions were magnetically stirred for 12 h at the ambient temperature of ~22 °C and the relative humidity of ~49% before electrospinning. The temperature and the relative humidity were measured using a Testo 610 handy temperature/humidity meter (Testo Ltd, Alton, UK). The physical properties of distilled water and PEO solutions such as surface tension, density, viscosity and electrical conductivity were measured (Table 1). Distilled water was used for calibration purposes as well as a reference material throughout the experiments. The surface tension was measured by using a Kruss Tensiometer K9 (Standard Wilhelmy's plate method). The density was obtained using a 25 ml standard density bottle and a chemical balance. The viscosity of each PEO solution was determined using a digital rotational viscometer (Brookfield, Harlow, UK). The electrical conductivity of the PEO solutions was obtained using a conductivity meter (Jenway

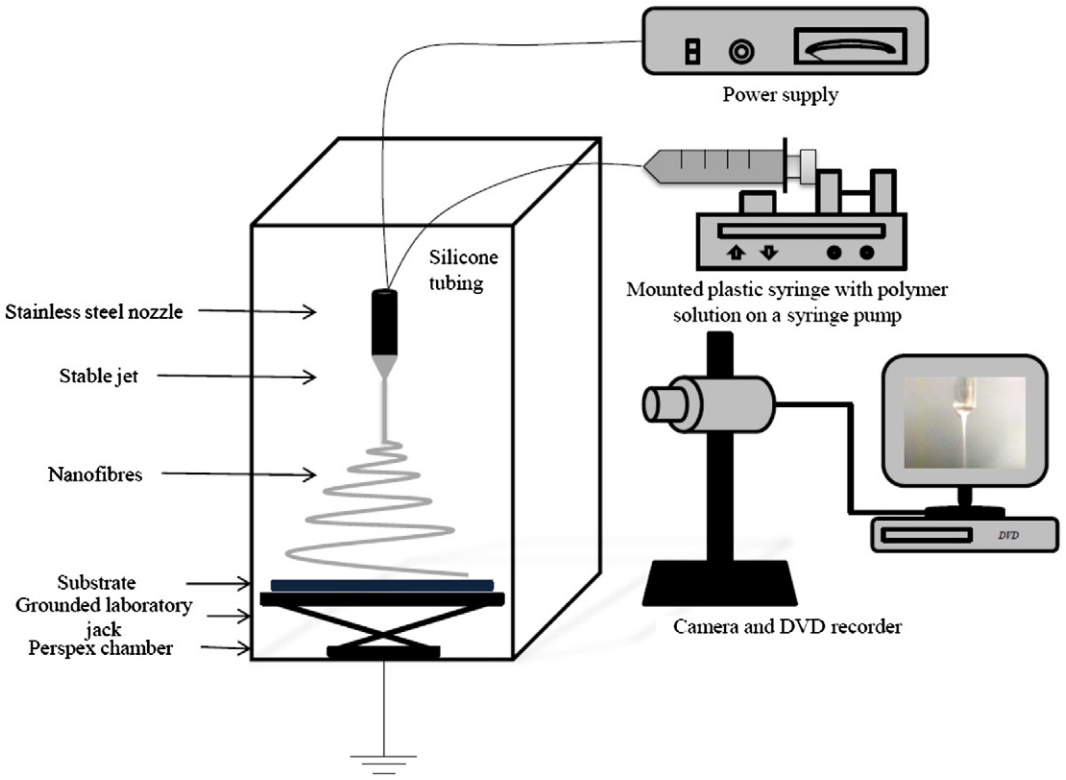

Fig. 1. Schematic illustration of the electrospinning process.

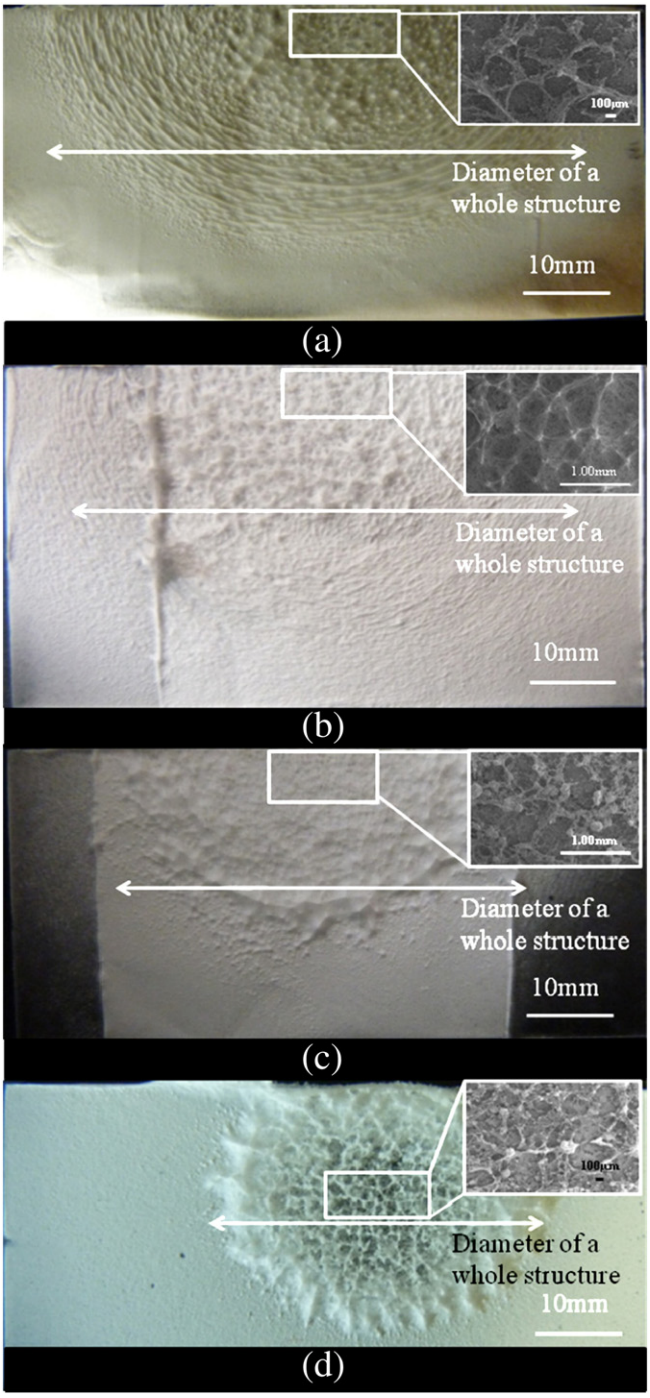

Fig. 2. Macro- and microstructures (inset) of self-assembled 3-D honeycomb-like nanofibrous structures obtained for different concentrations of PEO solution: (a) 12 wt.%, (b) 13 wt.%, (c) 14 wt.% and (d) 15 wt.%.

3540, Bibby Scientific Ltd, Stone, UK). All the physical properties of PEO solutions were measured five times and the average value was determined. During the measurements the equipment was cleaned with ethanol and distilled water before each reading to avoid errors.

2.2. Electrospinning

The experimental set-up of the electrospinning process used in this study is shown schematically in Fig. 1. The stainless steel nozzle with an inner diameter of 0.8 mm and an outer diameter of 1.1 mm was obtained from Stainless Steel Tubing (Stainless Tube & Needles Co Ltd, Tamworth, UK). One end of the nozzle was connected to a plastic syringe with silicone tubing (VWR International Ltd, Lutterworth, UK). The plastic syringe was clamped onto a syringe pump (Harvard Apparatus Ltd., Edenbridge, UK) to control the solution flow rate. The applied voltage was generated by a high voltage power supply (Glassman Europe Ltd, Bramley, UK) and connected to the nozzle to change the electric field strength between the orifice of the nozzle and the substrate. A stainless steel laboratory jack was used as a substrate supporter and it was grounded. An aluminium foil wrapped glass microscope slide or the slide on its own was placed on the surface of the stainless steel to collect the fibres. The working collection distance between the orifice of the nozzle and the substrate was varied to obtain different fibre morphologies during the study. The electrospinning process was carried out inside an insulated Perspex chamber. A video camera (LEICA S6D JVC-colour) linked to a DVD video recorder was used to observe the jetting phenomena during the process. Time of forming the structures was measured with a stop-watch (Table 1).

2.3. Characterisation of structures

The morphology of the structures produced was analysed visually using a high definition camera (iPhone 4S), a scanning electron microscope (SEM, Hitachi S-3400N, allows magnification of up to ×20,000) and a field-emission scanning electron microscope (FE-SEM, JSM-6301F, allows magnification of up to ×80,000). The glass and aluminium slides were coated with gold using a sputtering machine (Edwards sputter coater S1 50B) prior to observation under the SEM. The gold was sputtered for 120 s on each sample. The diameter of the nanofibres and the porous structures was determined by analysing the SEM images using the programme UTHSCSA (Image Tool Version 2, University of Texas, USA).

3. Results and discussion

3.1. Concentration of PEO

A flow rate of 20 μl/min and an applied voltage of 9.7 kV were used to process the 12 wt.%, 13 wt.%, 14 wt.% and 15 wt.% solutions. The aluminium substrate was placed below the nozzle at a distance of ~100 mm from the orifice of the nozzle to collect the electrospun nanofibres. For all three solutions jetting was stable under these conditions and the collection distance was set to 100 mm.

Fig. 2 shows the 3-D self-assembled macrostructures obtained using the 12 wt.%, 13 wt.%, 14 wt.% and 15 wt.% PEO solutions. The inset also shows the corresponding high magnification images of these. The diameter of the structures decreased with an increase in the concentration of PEO. For the 12 wt.%, the diameter is in the range of ~50–58 mm, for 13 wt.% it is ~48–55 mm, and for 14 wt.% it is ~40–45 mm. For the 15 wt.% of PEO solution the diameter decreased further to ~30–38 mm. The nanofibrous structures have nano-web meshes with well-defined boundaries. These are formed by self-alignment of the nanofibres during the electrospinning process. The boundaries consist of polymer beads which are more or less connected to each other to form the structures. The porous structure exhibits a polygonal like shape and runs to a depth of ~0.1–1.0 mm below the surface. The pore size of the honeycombs also changed with the PEO solution concentration and this is discussed in Section 3.4.

Fig. 3(a)–(d) shows the self-assembled honeycomb-like structures of the PEO solutions at higher magnifications. In each case bead on string morphology was observed (Fig. 3(e)–(h)). The bead diameter was irregular at each PEO concentration. The diameters of the beads are ~1.6–10.8 μm, ~1.1–2.5 μm, ~2.9–7.3 μm and ~1.4–2.2 μm for 12 wt.%, 13 wt.%, 14 wt.% and 15 wt.% PEO solutions, respectively. But the total numbers of beads decrease with increasing PEO concentration. These are similar to the observations of Fong et al. [33] and

Lee et al. [34]. The diameter of the nanofibres ranges from ~50 to 300 nm, ~43 to 454 nm, ~70 to 510 nm and ~90 to 600 nm for 12 wt.%, 13 wt.%, 14 wt.% and 15 wt.% PEO solutions, respectively. The most characteristic self-assembled honeycomb-like nanofibrous structure was achieved at 12 wt.% PEO solution (Fig. 3(a)). In addition, the time to form this structure decreased with the increase of viscosity of the PEO solution (Table 1). It was ~720 s for 15 wt.%, which is nearly half the time taken for the 12 wt.%. Fig. 3(i)–(j)

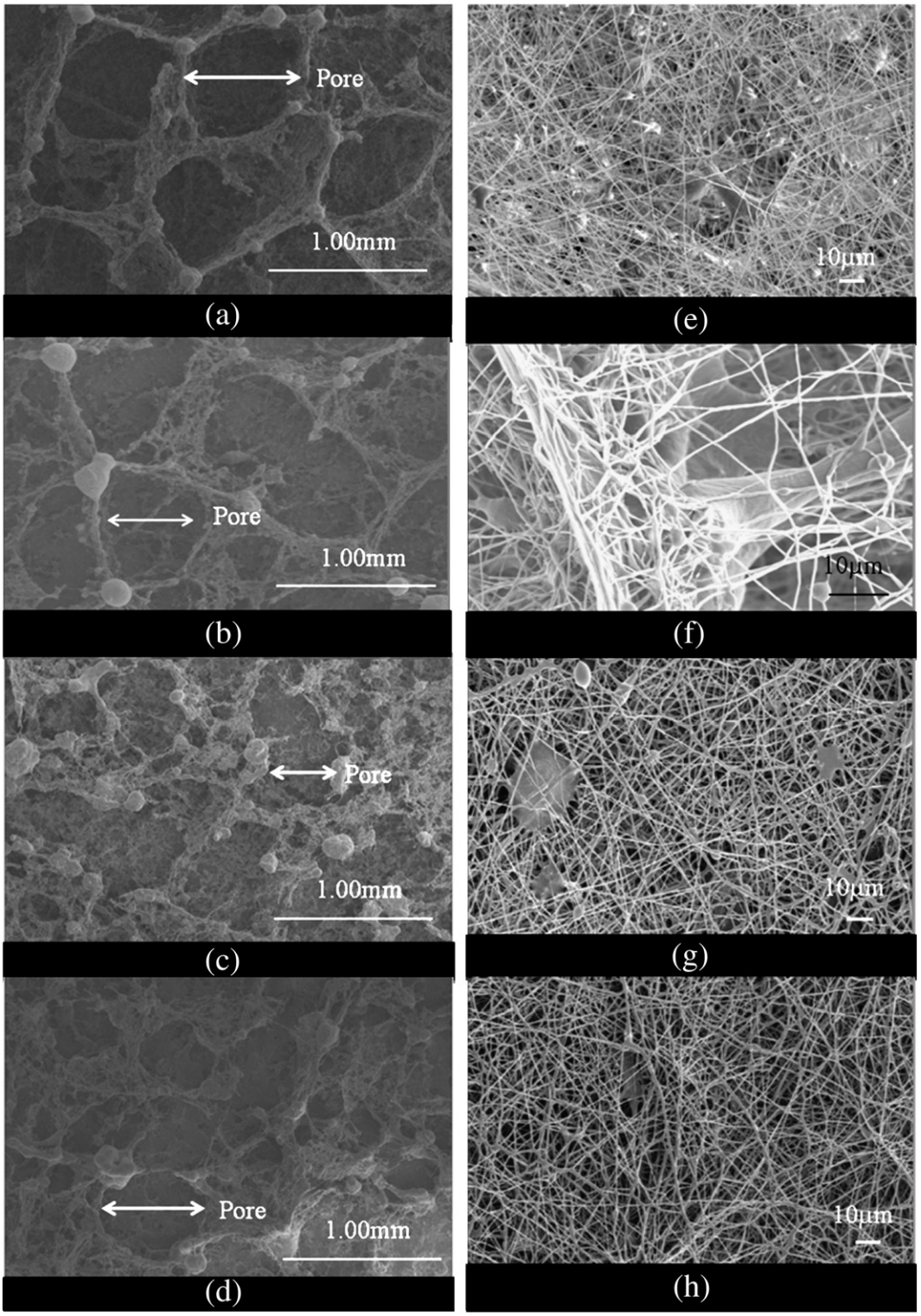

Fig. 3. Morphology of nanofibres and nanofibrous structures obtained from PEO solutions. (a), (b), (c) and (d) are low magnification images of the structures formed at 12 wt.%, 13 wt.%, 14 wt.% and 15 wt.% of PEO solution, respectively. (e), (f), (g) and (h) are high magnification images of the corresponding structures. (i) and (j) are 3-D honeycomb structures at 12 wt.% and 13 wt.%, respectively, obtained using a tilted SEM stage.

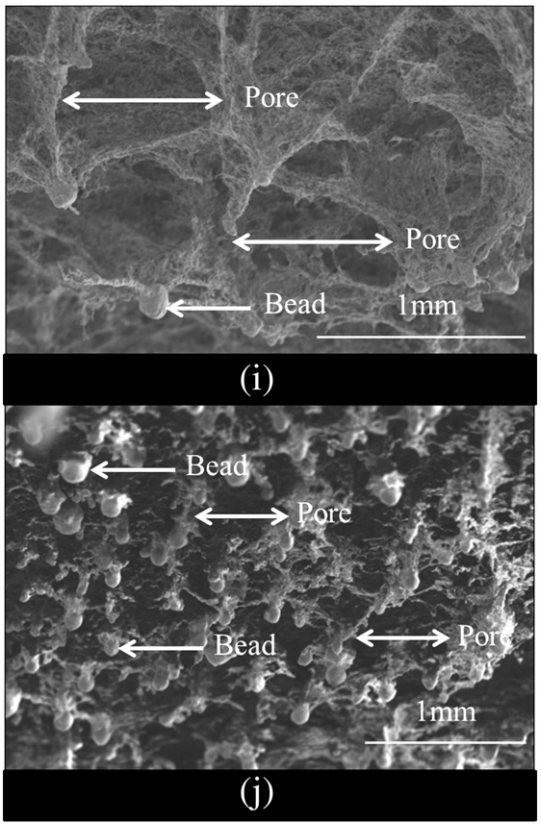

Fig. 3 (*continued*).

shows the 3D honeycomb structures obtained from tilted SEM stage (34°) for the 12 wt.% and 13 wt.% of PEO solutions, respectively. The porous structure exhibits a polygonal like shape and runs to a depth of ~0.1–1.0 mm below the surface.

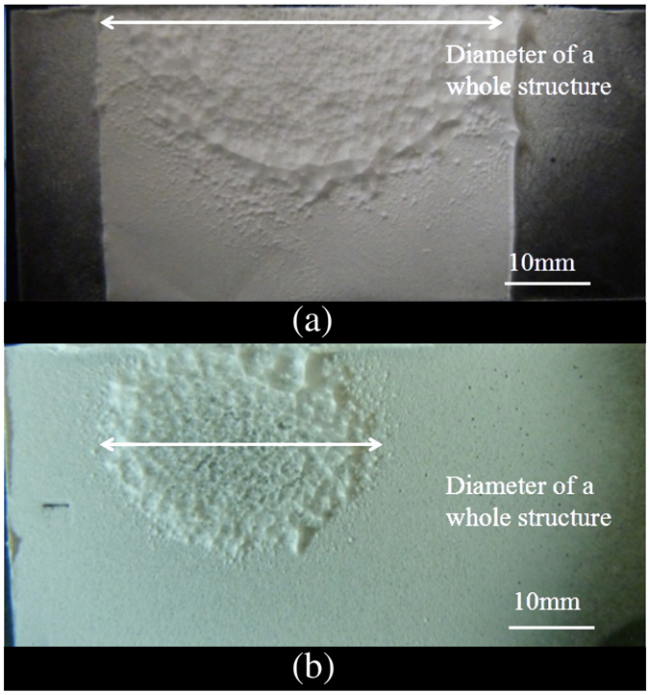

Fig. 4. Macrostructures of self-assembled 3-D honeycomb-like nanofibrous structures formed on different substrates using 14 wt.% of PEO (a) aluminium and (b) glass, at 9.7 kV, 20 μl/min flow rate, and 100 mm collection distance.

The polymer concentration has a significant effect on the size of polymer fibres and beads [31,33,35]. At a lower concentration of polymer, the electrospinning process generates a mixture of fibres and the beads. At higher concentrations, the nanofibres formed are regular and have cylindrical morphology [31] and the most likely reason for this could be the increase in viscosity [33]. In addition, the surface tension of the polymer solution depends on the type of polymer and the solvent used [33] and, generally, decreasing the surface tension of the polymer solution increases the diameter of the electrospun fibres [33]. However, in this work change in PEO concentration did not cause a dramatic difference to the surface tension (Table 1) in contrast to the viscosity which increased by over three orders of magnitudes and was the likely reason for the geometrical changes in the fibre structures.

During electrospinning the electric charges are carried by nanofibres and the beads. The quantity of charge depends on the size of the fibres and the beads and larger fibre and bead sizes have higher surface charges compared to the smaller counterparts [33]. These repel each other but are attracted to the grounded substrate during deposition. In addition, the fibres and the beads possess surface tension that wets and induces sticking together. The competing action of these two forces leads to self-alignment of nanofibres and consequently they are in a position to minimise their internal energy. Thus, this self-assembly leads to well defined characteristic 3-D nanofibrous structures. Over time, the charge density of the nanofibres increases and therefore the electrostatic repulsion to the incoming nanofibres increases to prevent the formation of a honeycomb structure. By invoking the model proposed by Yan et al. [36], when two or more nanofibres contact each other at a particular point the surface tension drives the nanofibres to join each other, on the other hand the electrostatic repulsive force keeps the fibres away and this leads to partial overlapping of the nanofibres. An increase in electrostatic repulsive force over time and the surface tension pushing the nanofibres to contact each other lead to the formation of the branched nanofibrous structures. The overlapping of these branched structures at a certain angle forms the honeycomb structures.

3.2. Collection substrate

An aluminium foil was wrapped around a standard glass microscope slide and used as one of the substrates, while the glass slide without wrapping was used for comparison. Fig. 4 shows the nanofibre morphologies of the 14 wt.% PEO solution deposited on these two substrates. The diameter of the whole honeycomb-like nanofibrous structure is ~45.6 mm and ~31.7 mm on the aluminium and the glass substrate, respectively, while keeping all other parameters the same. It is showing that varying the collection substrate material and thereby the substrate electrical conductivity can influence the size of the whole structure obtained. The structure on the insulating substrate is more compact than the structure on the more electrically conducting substrate. The results demonstrate that the electric field force strongly influences the structure configuration [37].

The pore size varied between ~63 μm and ~380 μm on the glass and ~150 μm and ~390 μm on the aluminium. Furthermore, the formed nanofibrous structures on the glass slide were more regular and visible than the structure formed on the aluminium (Fig. 4). These results demonstrated that the surface of the substrate has a significant effect on nanofibre self-assembly. Yan et al. [36] observed that larger pores were formed on an insulating substrate than on a conducting substrate. On the other hand, Thandavamoorthy et al. [32] also demonstrated that if a poor electrical conductor was used as a collector, then the formation of a well-defined three-dimensional honeycomb-like pattern will be enhanced. The evolution of pores in these types of structures is more complicated and dependent on many factors, as explained in Section 3.4.

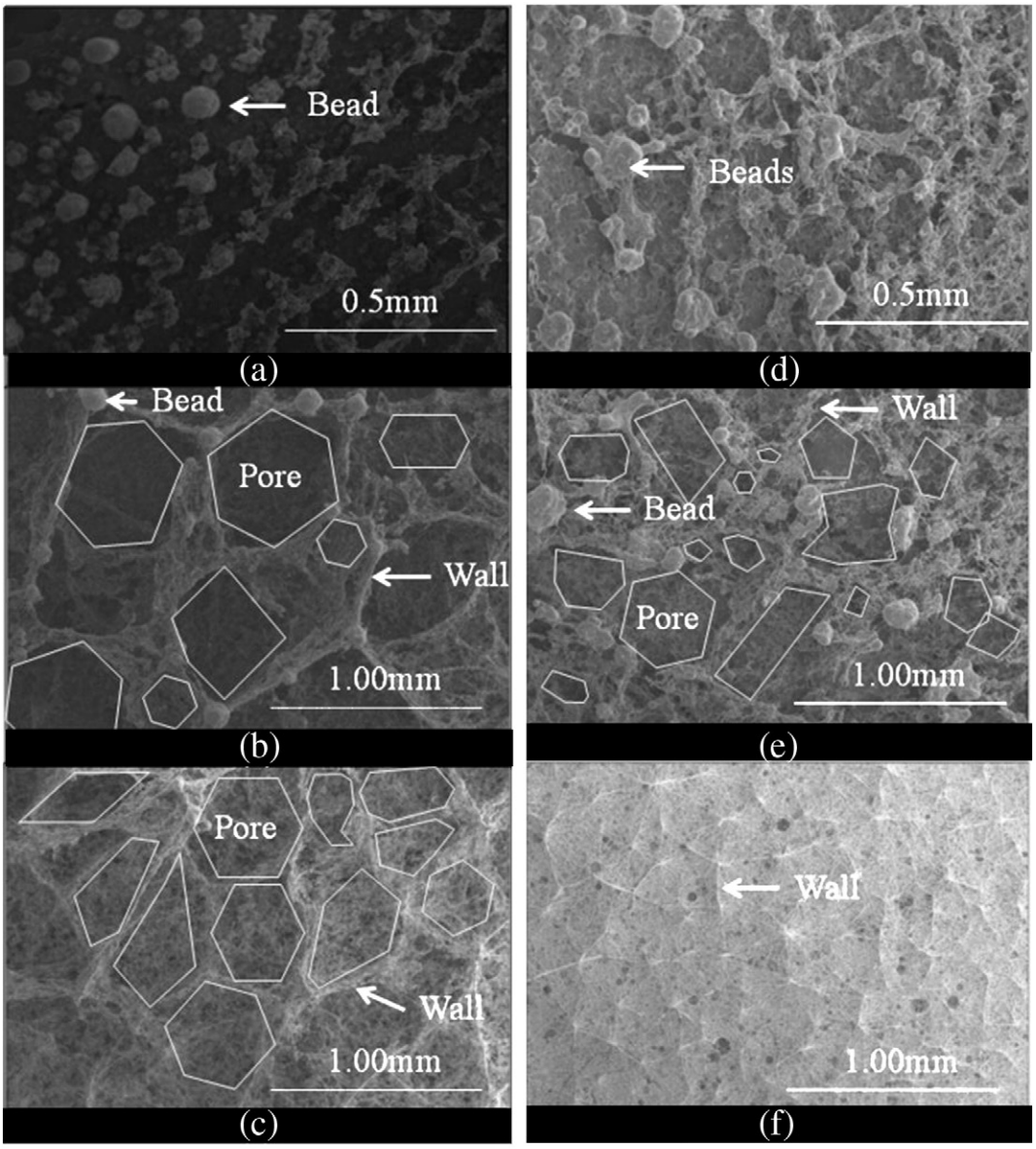

Fig. 5. SEM images of self-assembled 3-D honeycomb-like nanofibrous structures collected on aluminium with different collecting distances for PEO concentrations of 12 wt.% and 14 wt.% while keeping other parameters (listed above) constant. For 12 wt.% PEO, the collection distance was (a) 80 mm, (b) 85 mm and (c) 90 mm. For 14 wt.% of PEO corresponding values were (d) 95 mm, (e) 100 mm and (f) 150 mm.

3.3. Collection distance

The working or collection distance between the orifice of the nozzle and the substrate was varied to study its effect on the formation of the structures. For this purpose PEO solutions with a concentration of 12 wt.% and 14 wt.% were chosen. It was found that different concentrations of PEO solution have their optimum collection distance to form the most well-defined three-dimensional honeycomb-like structures. The 12 wt.% PEO solution starts to form the structure when the collection distance was ~80 mm. However, the 14 wt.% of PEO solution is able to generate the structure at ~100 mm (Fig. 5). Characteristic hexagonal pores were obtained when the collection distance was ~85 mm and ~100 mm for 12 wt.% and 14 wt.%, respectively (Fig. 5(b) and (e)). It is also clearly seen that the nanofibres haven't had enough time to evaporate and dry out to form the structures when the collection distance is below the optimum collection distance (Fig. 5(a) and (d)). On the contrary, increasing the collection distance above the optimum collection distance has allowed wet

nanofibres more time to dry out and form a shallow porous wall (Fig. 5(c) and (f)). Luo et al. [38] reported that increasing the collection distance decreased the electric field strength and this offers more spinning time for nanofibres thus leading to a solidification of the nanofibres before touching the substrate. These results are also consistent with the results of Yan et al. [36] who explained that increasing the collection distance offers more time for the evaporation of the solvent and eventually leads to the solidification of nanofibres.

Fig. 5(a) shows that walls of each pore are fragmentary and more pronounced beads were randomly distributed. This is because the collection distance hasn't given enough time for evaporation of the solvent from the wet nanofibres. A similar observation was found for the 14 wt.% PEO solution at a collection distance of 95 mm (Fig. 5(d)). At a concentration of 12 wt.%, the pore sizes varied between ~110 and 570 μm, ~185 and 582 μm and ~200 and 780 μm for collection distances of 80 mm, 85 mm and 90 mm, respectively. This shows that increasing the collection distance increases the pore sizes. In addition, when the concentration is 14 wt.%, the pore size is in the range of ~60–260 μm and ~110–460 μm for collection distances of 95 mm and 100 mm, respectively. These results demonstrate that the collection distance influences the pore size of the honeycomb-like structures. However, the pores are not apparent when the collection distance is 150 mm (Fig. 5(f)). In addition, it was also observed that by reducing the collection distance below the optimum value resulted in wetting of the substrates. A characteristic polygonal shape was formed when the collection distance is set at an optimum height.

3.4. Pore size

The pore size variation in the structure with different variables of the electrospinning process is shown in Fig. 6. It is noteworthy that the molecular weight of the PEO used will affect the characterisation of the fibres generated [38] and therefore the features of the honeycomb structure, in particular the pore size can be changed by selecting a PEO polymer with a different molecular weight. The 12 wt.% PEO solution shows an average pore size of 436 μm with a standard deviation of 184 μm. On the other hand, the 13 wt.% PEO shows an average pore size of 301 μm with a standard deviation of 168 μm. The 14 wt.% PEO solution results in an average pore size of 218 μm with a standard deviation of 59 μm. Thus, pore size is halved for this concentration compared to 12 wt.%. An average pore size of 224 μm was obtained for the 15 wt.% PEO solution, a slight increase compared with 14 wt.%. The addition of NaCl crystals to polymer solutions can give an increase in pore size [39]. In fact, here the average pore size increased by an order of magnitude. However, the addition of carbon nanotubes to polymer solutions showed a maximum porosity of the nanofibrous structures at a particular concentration [40]. Generally, the addition of NaCl to polymer solutions will increase the electrical conductivity due to incidental ionic species [41]. Similarly, addition of carbon nanotubes to polymer solution changes the solution conductivity and imparts a greater tensile force which increases stretching and splitting of the jet. This will have an effect on the spontaneous alignment of the structures. Consequently, this will have an influence on the pore size of the nanofibrous structures. Even though there are no NaCl crystals or carbon nanotubes in the polymer solutions used in the present work, an increase in electrical conductivity was observed with the increase in polymer concentrations (Table 1).

A pore size of 165 μm was obtained for the glass substrate while a pore size of 219 μm was observed for the aluminium substrate. Yang et al. [42] reported that the collection substrate has an influence on porosity and close arrangement of nanofibres. A decrease in pore size has been observed with decreasing electrospinning voltage [36]. Similarly, Touny and Bhaduri [43] reported more pore formation and the presence of larger diameter nanofibres with increasing

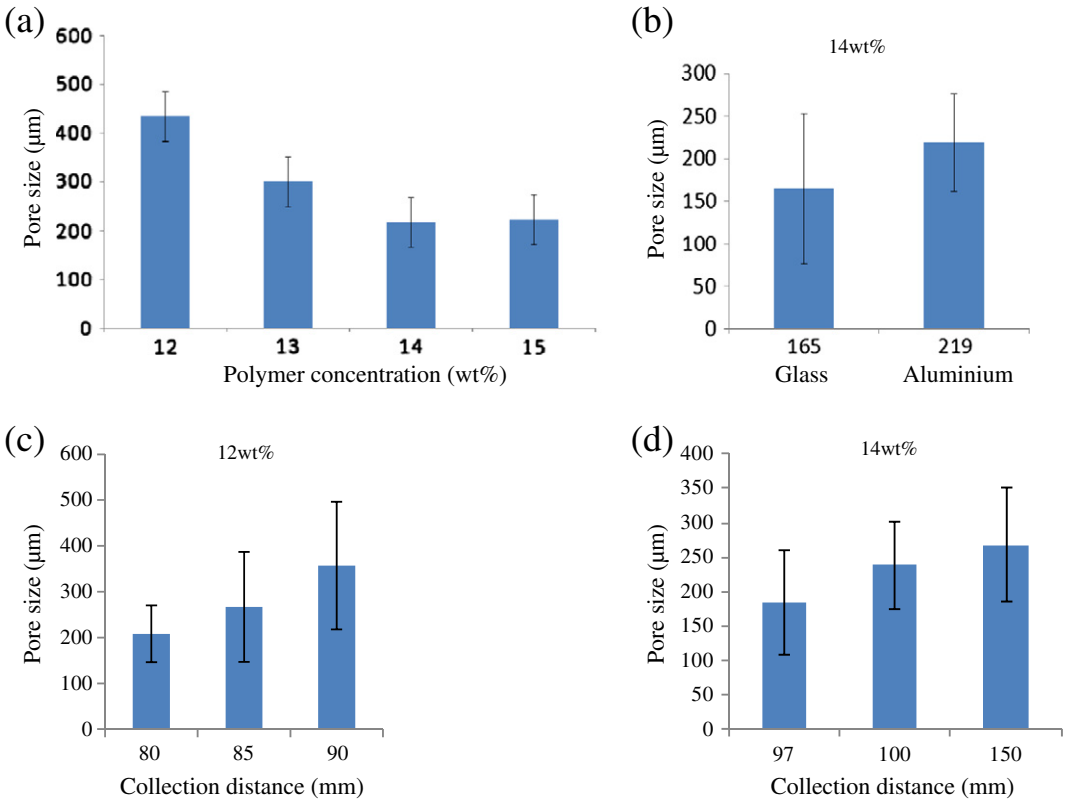

Fig. 6. Pore size in the honeycomb-like structures with respect to (a) concentration at 9.7 kV, 20 μl/min flow rate, and 100 mm collection distance; (b) substrate at 9.7 kV, 20 μl/min flow rate, and 100 mm collection distance; (c) and (d) collection distance, flow rate in both is 20 μl/min, for 12 wt.% PEO, 80 mm collection distance corresponds to 7.8 kV, 85 mm to 8.0 kV, and 90 mm to 8.1 kV; for 14 wt.% PEO, 97 mm collection distance corresponds to 9.3 kV, 100 mm to 9.7 kV, and 150 mm to 10.2 kV. In all cases stable jetting prevailed.

voltage. In this work, the spinning voltage is kept constant for the two cases illustrated in Fig. 6(b). However, the generated electric field lines will be different for the insulating substrate and conducting substrate, and create a different alignment and packing of fibres leading to a different variation in the pore size. The pore size variation with the collection distance is shown in Fig. 6(c) and (d) for 12 wt.% and 14 wt.% PEO. In both cases, increasing the collection distance increased the pore size. The pore size is varied from 210 μm to 360 μm at 12 wt.% PEO and 180 μm to 270 μm at 14 wt.% PEO. This is because at the shorter distance the nanofibres are wet and stick to each other. However, at the longer distance they are drier and do not merge together. In addition, the electrospinning process takes place over a shorter time period at the shorter working distances. Therefore, the dissipation of heat is less at shorter working distances and can lead to a change in the morphology of the nanofibres and the nanofibrous structures [43].

4. Conclusions

This investigation was carried out because well-defined unique honeycomb structures are promising candidates for cell adhesion, proliferation and differentiation. The effects of the electrospinning process control parameters and the concentration of polymer solution on the morphology of three-dimensional self-assembled PEO honeycomb-like structures have been investigated. The formation of the structures is influenced significantly by the concentration of PEO solution, collecting substrate and collection distance. The nanofibre diameter and the porosity have increased with the polymer concentration. The collection distance had a remarkable effect on the morphology of these nanofibrous structures where there is an optimum distance needed to form the honeycomb-like structures. For 12 wt.% of PEO solution the optimum distance was ~80–90 mm. On the contrary, for 14 wt.% of PEO solution the optimum distance was ~90–100 mm. The collecting substrate had a noticeable influence on the formed microstructures and these are mainly attributed to the competing action of electrostatic and surface tension forces.

References

[1] C.J. Luo, S.D. Stoyanov, E. Stride, E. Pelan, M.J. Edirisinghe, Chem. Soc. Rev. 41 (2012) 4708.
[2] S. Chaudhari, M.J. Srinivasan, J. Mater. Chem. 22 (2012) 23049.
[3] M. Li, J. Zhang, H. Zhang, Y. Liu, C. Wang, X. Xu, Y. Tang, B. Yang, Adv. Funct. Mater. 17 (2007) 3650.
[4] A.A. Sagade, K.R. Venkata, U. Mogera, S.J. George, A. Datta, G.U. Kulkarni, Adv. Mater. 25 (2012) 559.
[5] V. Vohra, U. Giovanelle, R. Tubino, H. Murata, C. Botta, ACS Nano 5 (2011) 5572.
[6] Y. Li, B.K. Guo, L.W. Ji, Z. Lin, G.J. Xu, Y. Liang, S. Zhang, O. Toprakci, Y. Hu, M. Alcoutlabi, Z.W. Zhang, Carbon 51 (2013) 185.
[7] Y. Li, C.W. Joo, J. Appl. Polym. Sci. 126 (2012) 252.
[8] S. Sinha-Ray, Y. Zhang, A.L. Yarin, Langmuir 27 (2011) 215.
[9] D.Y. Tu, S. Pagliara, R. Cingolani, D. Pisignano, Appl. Phys. Lett. 98 (2011) 023307.
[10] Y.C. Chui, Y. Chen, C.C. Kuo, S.H. Tung, T. Kakuchi, W.C. Chen, Appl. Mater. Interfaces 4 (2012) 3387.
[11] M.P. Francis, P.C. Sachs, P.A. Madurantakam, S.A. Sell, L.W. Elmore, G.L. Bowlin, S.E. Holt, J. Biomed. Mater. Res. A 100 (2012) 1716–1724.
[12] A. Welle, M. Kroger, M. Doring, K. Niederer, E. Pindel, I.S. Chronakis, Biomaterials 28 (2007) 2211.
[13] Z. Huang, H. Lee, E. Lee, S.K. Kang, J.M. Nam, M. Lee, Nat. Commun. 2 (2011) 459.
[14] N. Bhardwaj, S.C. Kundu, Biotechnol. Adv. 28 (2010) 325.
[15] J. George, Y. Kuboki, T. Miyata, Biotechnol. Bioeng. 95 (2006) 404.
[16] Q. Zhang, H. Luo, Y. Zhang, Y. Zhou, Z. Ye, W. Tan, M. Lang, Mater. Sci. Eng. C 33 (2013) 2094.
[17] P. Colombo, Phil. Trans. R. Soc. A 364 (2006) 109.
[18] K. Masuoka, T. Asazuma, M. Ishihara, M. Sato, H. Hattori, M. Ishihara, Y. Yoshihara, T. Matsui, B. Takase, M. Kikuchi, K. Nemoto, J. Biomed. Mater. Res. B 75 (2005) 177.
[19] Y. Kuboki, Q. Jin, H. Takita, J. Bone Joint Surg. Am. A 83 (2001) 105.
[20] J. Huang, S. Wang, C. Wei, Y. Xu, Y. Wang, J. Jin, G. Teng, Tissue Cell 43 (2011) 344.
[21] X. Guo, C.G. Elliot, Z. Li, Y. Xu, D.W. Hamilton, J. Guan, Biomacromolecules 13 (2012) 3262.
[22] H.B. Zhang, M.J. Edirisinghe, J. Huang, J. Am. Ceram. Soc. 89 (2006) 1870.
[23] N.M. Bedford, G.D. Winget, S. Punnamaraju, A.J. Steckl, Biomacromolecules 12 (2011) 778.
[24] A. Jaworek, A.J. Krupa, J. Aerosol Sci. 30 (1999) 873.
[25] C.J. Luo, E. Stride, S.D. Stoyanov, E. Pelan, M.J. Edirisinghe, J. Polym. Res. 18 (2011) 2515.
[26] C. Zhuo, R. Chu, R. Wu, Q. Wu, Biomacromolecules 12 (2011) 2617.
[27] V. Beachley, X. Wen, Mater. Sci. Eng. C 29 (2009) 663.
[28] J.A. Mathews, G.E. Wnek, D.G. Simpson, G.L. Bowlin, Biomacromolecules 3 (2002) 232.
[29] K. Desai, K. Kit, J. Li, S. Zivanovic, Biomacromolecules 9 (2008) 1000.
[30] G. Viswanathan, S. Murugesan, V. Pushparaj, O. Nalamasu, P.M. Ajayan, R.J. Linhardt, Biomacromolecules 7 (2006) 415.
[31] J.M. Deitzel, J. Kleinmeyer, D. Harris, N.C. Tan, Polymer 42 (2001) 261.
[32] S. Thandavamoorthy, N. Gobinath, S.S. Ramkumar, J. Appl. Polym. Sci. 101 (2006) 3121.
[33] H. Fong, I. Chun, D.H. Reneker, Polymer 40 (1999) 4585.
[34] K.H. Lee, H.Y. Kim, H.J. Bang, Y.H. Jung, S.H. Lee, Polymer 44 (2003) 4029.
[35] S.W. He, S.S. Li, Z.M. Hu, J.R. Yu, L. Chen, J. Zhu, J. Nanosci. Nanotechnol. 11 (2011) 1052.
[36] G. Yan, J. Yu, Y. Qiu, Z. Yi, J. Lu, Z. Zhou, Langmuir 27 (2011) 4285.
[37] J.C. Uecker, G.C. Tepper, J. Rosell-Llompart, Polymer 51 (2010) 5221.
[38] C.J. Luo, M. Nangrejo, M.J. Edirisinghe, Polymer 51 (2010) 1654.
[39] L.D. Wright, T. Andric, J.W. Freeman, Mater. Sci. Eng. C 31 (2011) 30.
[40] X.Z. Meng, W. Zheng, L. Li, Y.F. Zheng, Mater. Sci. Eng. C 30 (2010) 1014.
[41] A.L. Andrady, Science and Technology of Polymer Nanofibers, John Wiley & Sons, New Jersey, 2008.
[42] F. Yang, C.Y. Xu, M. Kotaki, S. Wang, S. Ramakrishma, J. Biomater. Sci. Polym. 12 (2004) 1483.
[43] A.H. Touny, S.Y. Bhaduri, Mater. Sci. Eng. C 30 (2010) 1304.

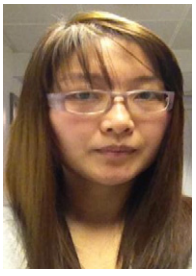

Tian Liang gained a BEng in Mechanical Engineering and a Master of Engineering Design degree from Brunel University, Uxbridge, UK, in 2007 and 2010, respectively. Currently she is a PhD student in the Department of Mechanical Engineering at University College London. She is working in the Biomaterials Processing and Forming Laboratory where her research focuses on electrospinning structures of polymeric materials.

Sunthar Mahalingam is a researcher and visiting lecturer in the Department of Mechanical Engineering at University College London (UCL). He received his PhD in electrohydrodynamic processing of thin films at UCL in 2008, and his current research areas are innovative-manufacturing, characterisation of structural–functional and bio-materials.

Mohan Edirisinghe DSc holds the Bonfield Chair of Biomaterials in the Department of Mechanical Engineering at University College London. He has published over 300 journal papers and his most recent research is on advanced jet techniques for the preparation of novel biostructures including microbubbles and drug delivery capsules. He has been awarded many prizes for his research including the 2012 UK Biomaterials Society President's prize.